DEPARTMENT OF
ENERGY, MINES AND RESOURCES
MINES BRANCH
OTTAWA

*Mines Branch Program*
*on Environmental Improvement*

# *SAMPLING AND CHARACTERIZATION OF CUPOLA EMISSIONS*



R. D. WARDA AND R. K. BUHR

PHYSICAL METALLURGY DIVISION

JULY 1973

Research Report R 266

Price: $1.00

Available by mail from Information Canada, Ottawa, K1A 0S9
and at the following Information Canada bookshops:

HALIFAX
1683 Barrington Street

MONTREAL
640 St. Catherine Street West

OTTAWA
171 Slater Street

TORONTO
221 Yonge Street

WINNIPEG
393 Portage Avenue

VANCOUVER
800 Granville Street

or through your bookseller

Price: $1.00 Catalogue No M38-1/266

Price subject to change without notice

Information Canada
Ottawa, 1974

Mines Branch Research Report R 266

# SAMPLING AND CHARACTERIZATION OF CUPOLA EMISSIONS

by

R. D. Warda* and R. K. Buhr**

## ABSTRACT

This report is divided into two parts, the first dealing with the sampling technique employed and its reliability and, the second, with the actual results obtained at six iron foundries. The stack sampling method adopted was originally used extensively for the sampling of flue gases from combustion processes. Modifications were made to make the sampling trains more rugged, portable, and responsive to the rapidly changing conditions in a cupola stack. The equipment was field tested over a 12-week period during which detailed measurements were made on the emissions produced by six iron foundry cupolas.

The reliability and practicability of the method used was assessed by statistical analyses and materials balance calculations. It is shown that repetitive sampling is mandatory if statistically significant results are to be obtained.

Analysis of both the gaseous and particulate effluent data indicate the following:

(1) amount and type of both gaseous and particulate effluent vary significantly with the design and operation of the cupola,

(2) gaseous effluent characteristics are affected primarily by the ratio of coke: total air and by gas temperatures at the point of mixing with charge door air,

(3) regarding particulate effluent, the cupola is both a transmitter and a generator, the transmitted component usually predominating, and

---

*Research Scientist, and **Head, Foundry Section, Physical Metallurgy Division, Mines Branch, Department of Energy, Mines and Resources, Ottawa, Canada.

(4) suggestions made during testing both to reduce and identify the transmitted component of the particulate effluent were highly successful.

The results emphasize the necessity for detailed emission studies on individual cupolas in order to supply reliable information to those concerned with pollution abatement in the iron foundry industry.

Direction des mines
Rapport de recherches R 266

# L'ÉCHANTILLONNAGE ET LA CARACTÉRISATION DES EMISSIONS DU CUBILOT

by

R. D. Warda* et R. K. Buhr**

## RÉSUMÉ

Les auteurs ont divisé ce rapport en deux parties, traitant tout d'abord de la technique d'échantillonnage qu'ils ont employé, et deuxièmement traitant des résultats réels qu'ils ont obtenus à six fonderies de fonte. La méthode adoptée d'échantillonnage de fumée a été originalement utilisée extensivement pour l'échantillonnage des gaz de carneau des procédés de combustion. Ils ont fait des modifications pour rendre les trains d'échantillonnage plus rugneux, plus portatifs et plus responsifs aux changements rapides des conditions rencontrées dans une cheminée de cubilot. Ils ont mis à l'essai l'équipement pendant une période de 12 semaines, durant ce temps, ils ont pris des mesures détaillées sur les émissions produites par six cubilots de fonderie de fonte.

Les auteurs ont évalué la crédibilité et la practicabilité de la méthode utilisée par les analyses statistiques et par les calculs de balance de matériel. Ils ont montré que la répétition de l'échantillonnage est nécessaire s'ils veulent obtenir des résultats significatifs du point de vue de la statistique.

L'analyse des données de l'effluent gazeux et particulaire indique les faits suivants:

(1) le montant et le type de l'effluent gazeux et particulaire varient significativement selon le dessin et le fonctionnement du cubilot,

(2) les caractéristiques de l'effluent gazeux sont principalement affectées par le coke: les rapports de l'air total, et par les températures de gaz au-dessus de la porte pour le chargement,

*Chercheur scientifique, et **Chef, Section de la fonderie, Division de la métallurgie physique, Direction des mines, ministére de l'Énergie, des Mines et des Ressources, Ottawa, Canada.

(3) concernant l'effluent particulaire, le cubilot est à la fois, un transmetteur et un générateur, le composant transmis est ordinairement prédominant, et

(4) les suggestions faites durant les essais pour réduire et pour identifier le composant transmis de l'effluent particulaire ont été une très grande réussite.

D'après les résultats, les auteurs ont fait voir la nécessité des études détaillées sur les émissions des cubilots individuels afin de pourvoir fournir des renseignements sûrs à ceux qui s'occupent de réduire la pollution dans l'industrie de fonderie de fonte.

General Introduction

At present, foundrymen are confronted by two main problems in their attempt to respond to increasingly stringent regulations on air pollution. The individual foundryman has little idea of the nature or extent of the emissions from his plant, so he can neither establish the level of emission of his plant in terms of currently acceptable levels, nor can he deal knowledgeably with the problem of reducing emissions that may be too high. In attempting to determine the emissions he is confronted by the problem of the questionable reliability of current methods of sampling.

A reliable and practicable method has been developed for measuring and assessing particulate and gaseous emissions from iron foundry cupolas, and is described in the first part of this paper. In the second part detailed characteristics of gaseous and particulate emissions from six iron foundry cupolas are presented and correlated with certain operating practices.

# PART I

# A METHOD FOR SAMPLING CUPOLA EMISSIONS

## Introduction

This part describes a reliable, practicable method for measuring and assessing particulate and gaseous emissions produced by iron foundry cupolas. Although attention is devoted primarily to sampling raw exhaust gas in the cupola stack above the charge door, sampling requirements downstream from emission control devices are also considered. The methodology encompasses not only the actual techniques of sampling, but the recording and assessing of all cupola operating parameters. Reliability and practicability are assessed by the application of statistical analyses and materials balance calculations to data collected during detailed studies of cupola emissions conducted at six iron foundries in the Province of Ontario.

## General Test Procedures

### Duration of Tests

Daily testing programs were conducted for two weeks at each of five foundries, and for one week at the sixth. The length of the daily test period at any foundry depended upon the melt schedule, which was between 1.5 and 8 hours, and the following conditions:

1) no sampling during the first and last 15 minutes of the melt schedule,
2) equal time at each sampling point,
3) all points in the test cross-section to be sampled during a test, and
4) sampling time at each point either to equal or exceed the charge cycle time.

Table 1 summarizes the test parameters for all the foundries tested.

## Location of Test Cross-Section and Sampling Points

All tests were conducted in the cupola stack above the charge door. Depending on limitations imposed by access or downstream flow disturbances, the distance between the charge door and the test cross-section varied from 2.5 to 6 stack diameters. The test cross-section was subdivided into either 3 or 5 equal concentric areas. Two mutually perpendicular probes were used to sample each sub-area at 4 locations, i.e., 2 per probe. The sampling stations for each probe, given as a percentage of the stack diameter from the circumference to the test point, are as shown in Table 2.

TABLE 1

Summary of Test Parameters

| Foundry | No. of Test Days | No. of Tests | Av. Test Time (Min) | No. of Stations Probed/ Test | No. of Charges/ Station | % Time Wind On |
|---|---|---|---|---|---|---|
| A | 8 | 22 | 48.5 | 6 | 2.0 | 100 |
| B | 7 | 22 | 101.5 | 6 | 2.2 | 99.6 |
| C | 8 | 21 | 78.8 | 6 | 1.7 | 87.1 |
| D | 9 | 26 | 93.4 | 10 | N.A. | 100 |
| E | 7 | 14 | 119.1 | 10 | 1.4 | 78.9 |
| F | 4 | 8 | 60 | 6 | 1.0 | 88.7 |

TABLE 2

Location of Stack Sampling Stations

(% of Stack Diameter)

| Station No. | 1 | 2 | 3 | 4 | 5 | 6 | 7 | 8 | 9 | 10 |
|---|---|---|---|---|---|---|---|---|---|---|
| Number of Equal Areas | | | | | | | | | | |
| 3 | 4.4 | 14.7 | 29.4 | 70.6 | 85.3 | 95.6 | | | | |
| 5 | 2.2 | 8.2 | 14.5 | 22.7 | 34.4 | 65.6 | 77.3 | 85.5 | 91.8 | 97.8 |

Access to the test cross-section was achieved through two 3 x 6-inch holes in the stack at the appropriate locations. The diametral probe traces and the discrete sampling points were defined by a calibrated probe-track welded to the outer cupola shell. These features are shown in Figure 1 which also illustrates the labelling and location of the two probes with respect to the charge door which was directly under probe A.

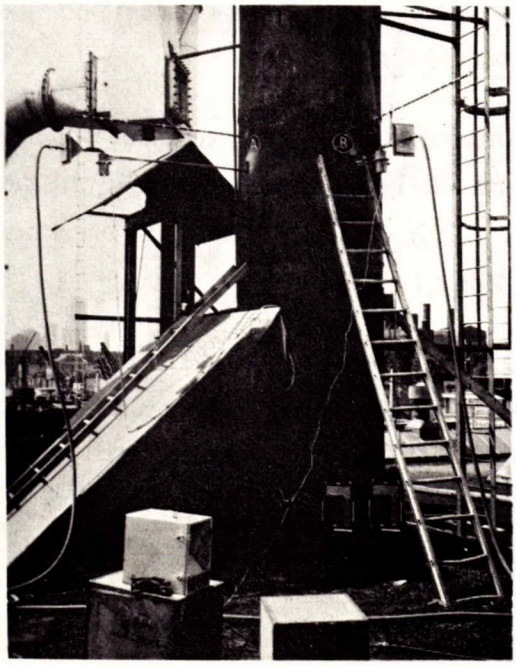

Figure 1. Test Installation at a Foundry.

## Scope of Tests

Each test consisted of the simultaneous measurement of velocity, temperature, and composition of the stack gas, and the continuous isokinetic collection of particulate. Cupola charging and operating practices were observed and recorded in a log book for subsequent correlation with emission measurements.

## Treatment of Data

Critical emission parameters are described by their mean values ($\bar{X}$), standard deviations (s), and coefficients of variation ($V = (s/\bar{X}) \times 100$). The significance of sources of variation are determined using the F-test. All sources of variation for which the F-test yielded a probability of less than 5 per cent were considered significant. Material balance calculations were used to test for bias.

# Part A - Measurement of Stack Gas Temperature and Velocity of Stack Gas

## Equipment and Methods

Gas temperatures at each sample point were measured continuously with chromel-alumel type K thermocouples sheathed in stainless steel. The EMF outputs from the two thermocouples were recorded autographically.

Gas velocities at each sample point were measured by stainless steel standard-type Pitot tubes and inclined manometers. Velocity pressure readings were taken at one-minute intervals and converted to feet per minute (FPM) at 70°F by means of isothermal conversion plots of the equation:

$$V_o = 9.22\sqrt{H/T_s}$$

where $V_o$ = velocity in fpm at 70°F.

$H$ = velocity pressure in inches W.G.

$T_s$ = gas temperature in °R.

Measurements of the absolute pressure and composition of the stack gas indicated that the maximum bias resulting from the use of this simplified equation would be less than 3 per cent.

## Results

Temperature measurements at each of the six foundries are summarized in Figure 2, in which the stack gas temperature is described by the per cent of time during an individual test that it exceeds a given value. The results from four of the foundries are summarized without any discrimination between individual tests. At the remaining two foundries, differentiation between certain tests was required in order to illustrate changes in temperature occurring either during melting or because of changes in cupola operation.

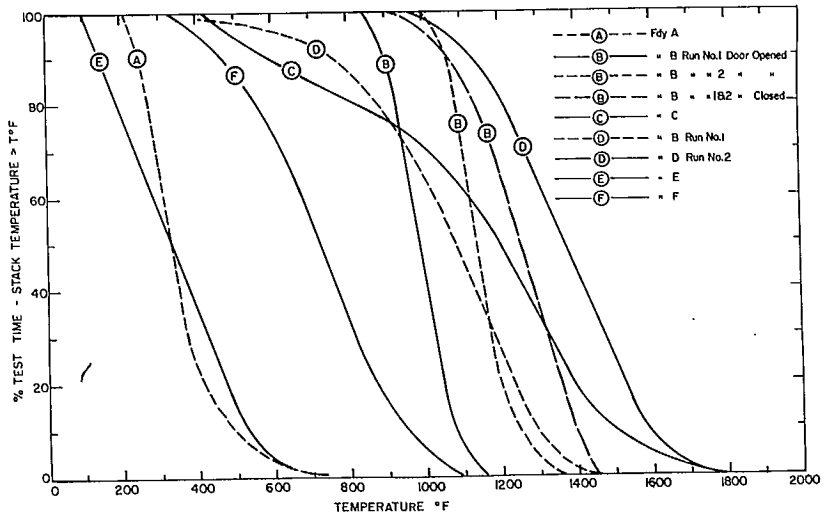


Figure 2. Distribution of Stack Temperatures as a Fraction of Test Times.

Velocity measurements and resultant stack gas flow rates are summarized in Table 3. The statistical parameters show the distribution of average stack velocities, each of which consists of the average of the velocities measured at all points sampled during a test.

TABLE 3

Summary of Stack Gas Velocities and Flow Rates

| Foundry | Stack Velocity $\bar{X}$ (fpm) | s (fpm) | V (%) | Stack Area ($Ft^2$) | Stack Flow Rate (SCFM) |
|---|---|---|---|---|---|
| A-1 (1) | 912 | 57 | 6.2 | 12.6 | 11,500 |
| A-2 (1) | 780 | N.A. | N.A. | 12.6 | 9,800 |
| A-3 (1) | 1123 | N.A. | N.A. | 12.6 | 14,200 |
| B-1 (2) | 1016 | 47 | 4.7 | 18.3 | 18,500 |
| B-ACD(2) | 755 | 35 | 4.7 | 18.3 | 13,900 |
| C | 786 | 67 | 8.5 | 14.7 | 11,600 |
| D | 412 | 40 | 9.7 | 13.0 | 5,350 |
| E-1 (3) | 1076 | 39 | 3.6 | 12.6 | 13,600 |
| E-2 (3) | 1397 | 77 | 5.5 | 12.6 | 17,600 |
| F | 599 | 38 | 6.8 | 10.55 | 5,900 |

(1) The designations A-1, A-2, and A-3 refer to the use of charge materials of normal, low, and high permeability respectively.

(2) B-1 refers to the first test of each melt schedule, B-ACD indicates the operation of an automatic charge door closing.

(3) E-1 and E-2 refer to identical adjacent cupolas.

The variation of temperature and velocity during sampling are of particular importance to the problem of isokinetic particulate collection, therefore temperature and velocity profiles for both probes are shown in Figure 3. The standard deviation bars at each test point illustrate the variation of velocity and temperature with time during a single test.

Variance tests were applied to all velocity and temperature measurements. Both temperature and velocity variations between foundries were highly significant. Temperature varied significantly with time from the start of melting at foundries B and D; corresponding velocity variations were not significant. Significant day-to-day variations in temperature occurred at 4 foundries (B, C, D, and E), but at only one foundry (A) were there variations in velocity. Changes in cupola operation described in the footnotes to Table 3 produced significant variations in both temperature and velocity at foundry B but in velocity only at foundries A and E. Velocity varied significantly with probe position at foundries A, C, D, and E; temperature varied significantly only at foundry C.

## Part B - Measurement of Particulate Emissions

Particulate emissions are characterized primarily by two parameters: the rate at which they are produced and their size distribution. This part is concerned essentially with the first parameter; the second is measured only to the extent that the size distribution was determined in situ by the collecting apparatus. Methods and results of more detailed size distribution analyses are reported in Part II.

### Equipment and Methods

Particulate samples were collected by two sampling trains which were similar to those used extensively by personnel of the Canadian Combustion Research Laboratory for sampling flue gases from a wide range of combustion processes. The main features of the probe train are shown in Figure 4. The probe, cyclone separator, and filter holder were constructed of type 304 stainless steel. Glass fibre filters were used to avoid degradation by exposure to elevated temperatures.

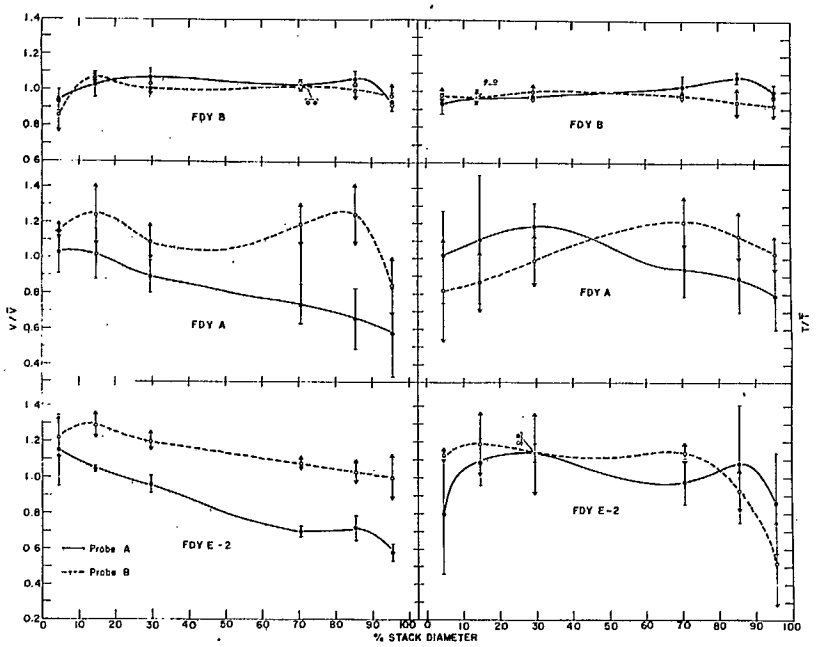


Figure 3. Stack Gas Velocity and Temperature Profiles for Both Probes. Velocity and Temperature are the Average of all Values Obtained by Both Probes.

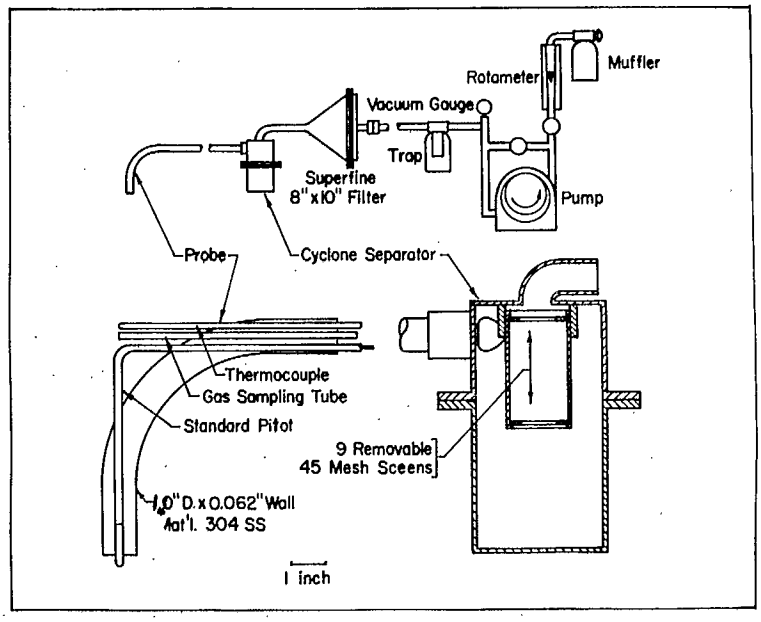


Figure 4. Details of Particulate Sampling Train.

Gas flow rate in the sampling train was controlled by the operation of two valves - one on a pump by-pass circuit and one on the pump exhaust downstream from the rotameter. The second valve also performed the important function of attenuating pressure pulsations which would otherwise introduce a bias into the rotameter readings. The rotameter calibration was checked by the Standards Laboratory of the Department of Corporate and Consumer Affairs and found to be accurate to within 3% between 0.46 and 4.6 SCFM for air at $70^{0}$F. It was assumed that departures of exhaust gas temperature from $70^{0}$F and gas density from that of air did not cause appreciable error in flow measurement.

With the exception of tests designed to measure peak emission rates, each test consisted of the continuous, simultaneous collection of particulate by both sampling trains. Details of the number and positions of the stations sampled by each probe during a test and the sampling interval have been described previously.

Isokinetic sampling conditions were maintained throughout both the continuous and intermittent tests to the extent permitted by variations of stack gas conditions. The sample-train flow rate corresponding to isokinetic conditions was determined at one-minute intervals by means of the isothermal velocity conversion graphs re-scaled to account for the cross sectional area of the probe. Deviations from isokinetic conditions exceeding 5 per cent were corrected and the correction times were recorded to facilitate calculation of the total volume of gas sampled during a test.

At the conclusion of each test, the sampling train was disassembled and the cyclone filter section was taken to a draft- and dust-free location where all loose and adherent dust from the cyclone separator and the screens was sealed in a labelled bottle. The glass fibre filter was carefully removed from the holder, folded to protect the adherent dust, and sealed in an envelope. A gram-matic balance, accurate to within 0.1 mg, was used to tare individual sample bottles and filters and to weigh them after accumulation of samples.

Subsequent size analyses indicated that 97 per cent of the dust collected in the cyclone was plus 25-micron, the remainder being minus 25 plus 1-micron. All the dust collected in the filter was sub-micron.

## Results

The results of the continuous particulate emission tests performed at the six foundries are summarized in Table 4. Particulate emission rates, expressed as pounds of total particulate per ton of metal charged, are shown as they were accumulated chronologically at each foundry. The number of samples "n" contributing to each result is the sum of the samples collected by both probes. The numbers n (10%), n (25%), and n (50%) indicate the number of samples required at each foundry if the true mean is to deviate from the sample mean by less than the amounts indicated in parentheses. Results of the continuous and intermittent emission tests are combined in Table 5 to illustrate the variation of particulate emission rate during a charging cycle.

The large variations in the results presented in Table 4 indicate the existence of sources of significant variation within the foundries. Accordingly, all particulate emission data were subjected to the same variance tests which were applied to the gas temperature and velocity results. The results of these tests not only confirmed that foundry-to-foundry variations were highly significant but that significant variations occurred from day to day at foundries A, B, C, and E, and, because of changes in cupola operation, at foundry A. The changes in cupola operating practice, instituted and studied at foundry A, and their influence on particulate emission rates are shown in Table 6.

Table 4

Summary of Dust Production Rates

| Foundry | No. of Days | No. of Tests (n) | $\bar{X}$, Lb/Ton | s, Lb/Ton | V, % | No. of Tests Required* for 95% Confidence Limits of ±50% | ±25% | ±10% |
|---|---|---|---|---|---|---|---|---|
| A | 1 | 2 | 75.5 | 13.5 | 17.9 | | | |
| | 2 | 4 | 64.0 | 17.0 | 26.6 | | | |
| | 4 | 12 | 47.4 | 15.7 | 33.1 | | | |
| | 8 | 22 | 44.9 | 13.5 | 30.2 | 4 | 8 | 38 |
| B | 1 | 2 | 10.0 | 1.70 | 17 | | | |
| | 2 | 4 | 10.75 | 1.42 | 13.2 | | | |
| | 4 | 12 | 14.31 | 3.89 | 27.2 | | | |
| | | 22 | 15.48 | 3.88 | 25.1 | 4 | 6 | 26 |
| C | 1 | 2 | 11.1 | 3.50 | 31.5 | | | |
| | 2 | 6 | 19.4 | 6.46 | 33.3 | | | |
| | 4 | 12 | 19.8 | 7.12 | 36.0 | | | |
| | 8 | 21 | 17.9 | 7.33 | 40.9 | 6 | 12 | 66 |
| D | 1 | 2 | 11.75 | 4.24 | 36.1 | | | |
| | 2 | 6 | 10.2 | 3.15 | 30.9 | | | |
| | 4 | 12 | 9.7 | 2.73 | 28.1 | | | |
| | 9 | 26 | 8.2 | 2.63 | 32.1 | 4 | 8 | 42 |
| E | 1 | 2 | 53.0 | 7.00 | 13.2 | | | |
| | 2 | 4 | 43.0 | 11.4 | 26.4 | | | |
| | 4 | 8 | 37.8 | 9.73 | 25.8 | | | |
| | 7 | 14 | 34.1 | 9.40 | 27.5 | 4 | 8 | 32 |
| F | 1 | 2 | 3.8 | 0.19 | 3.8 | | | |
| | 2 | 4 | 4.2 | 0.64 | 15.2 | | | |
| | 4 | 8 | 4.8 | 1.16 | 24.1 | 4 | 6 | 26 |

*n was calculated using the confidence interval relationship for true means

$$\mu = \bar{X} \pm t_{0.95} \frac{s}{\sqrt{n}}$$

where $\mu$ is the true mean, $t_{0.95}$ is the t-statistic for a 95% confidence interval; X, V, s, and n have been defined on pp. 4 and 10.

Variance analyses of the results of the changes in charging practice indicated that the introduction of a screen on the foundry returns system caused a highly significant reduction in emission rates. No other changes in charging practice were significant.

TABLE 5

Comparison of Dust Production Rates During Charge Cycle

| Foundry | Dust Production Rate (Lb/Min) | | | Ratio | |
|---|---|---|---|---|---|
| | Peak | Off-Peak | Average | Peak/Off Peak | Peak/Average |
| A | 12.5 | 4.2 | 5.24 | 3.0 | 2.4 |
| B | 13.8 | 0.9 | 1.96 | 15.3 | 7.0 |
| C | 4.1 | 1.0 | 1.31 | 4.1 | 3.1 |
| D | 1.3 | 0.45 | 0.60 | 2.9 | 2.2 |

Sampling error was another source of variation investigated. The assessment of the significance of this source of variation was made by a comparison of the variability of samples collected under controlled conditions* with that of samples collected at individual cupolas. Table 7 describes the conditions under which the sampling error determinations were made and presents the results as a ratio of the dust weights collected by the simultaneous operation of the two probes placed adjacent to each other in the dust stream. The handling and weighing of dust-laden filters were also checked as sources of error by reweighing a group of filters selected at random. The ratio of the first weight to the second was 1.019 ± 0.052.

---

*A cupola stack simulator 12 in. in diameter has been constructed by the authors for studying the collection of particulate from hot gases.

Table 6

Influence of Charging Practice on Dust Production at Foundry A

| Period | Dust Production Rate | | Remarks |
|---|---|---|---|
| | $\bar{X}$, (Lb/Ton) | s, (Lb/Ton) | |
| Days 1, 2, and 3 | 51.8 | 17.6 | Standard charging practice, scrap small and rusty. |
| Days 4 and 5, Runs 1 and 2 | 43.6 | 5.5 | As during days 1, 2, and 3 except that scrap consisted of large plates with less rust. |
| Day 5, Run 3 | 25.0 | 5.0 | As during days 4 and 5 except that loose sand was removed from foundry returns by a screen. |
| Day 6 | 43.5 | 3.5 | As during days 4 and 5 (Runs 1 and 2) except that plate scrap was completely free of rust. |
| Day 8 | 18.5 | 1.5 | As during day 5 (Run 3) except that extra precautions were taken to prevent charging of loose sand, rust, and coke fines. |

Table 7

Test of Sampling Errors

| Gas Velocity (FPM) | Dust Loading, (Grains/SCF) | Mean Sample Size, (g) | % Off Isokinetic | | Wt A/Wt B |
|---|---|---|---|---|---|
| | | | A | B | |
| 392 | 1.90 | 2.70 | 0 | 0 | 1.0185 ± 0.0200 |
| 795 | 0.95 | 5.0 | 0 | 0 | 1.0413 ± 0.0200 |
| 795 | 0.95 | 4.1 | 0 | -20 | 1.0647 ± 0.0244 |
| 795 | 0.95 | 4.3 | 0 | +20 | 1.0064 ± 0.0282 |

## Part C - Measurement of Gaseous Emissions

In a cupola, in which a carbonaceous non-volatile fuel is burned, the exhaust gas components of primary concern are CO, $SO_X$, and $NO_X$. However, the measurement of $CO_2$ and $O_2$ can provide useful data for determining not only the air/fuel ratio in the combustion zone but the degree of dilution of the combustion product gases by air drawn in through the charge opening. Measurements of CO, $SO_X$ and $NO_X$ were therefore made to characterize the gaseous pollutants; measurements of $CO_2$ and $O_2$ were made to characterize the system from which the pollutants are emitted.

### Equipment and Methods

Gaseous emission sampling was performed simultaneously with the emission measurements described in A and B. Only one gas sampling train was used, so sampling was conducted alternately by each probe. During a test, stack gas was withdrawn continuously at 0.5 SCFM through a stainless steel tube which extended to the tip of the particulate sampling probe. Before entering the various sampling units, the gas was filtered and dried by passing it through packed columns of glass wool and indicating silica gel. The clean dry gas then entered the analyzing system which provided continuous, autographic measurement of CO and $CO_2$ concentrations[1]. Orsat samples were drawn off through a tee in the gas line just upstream from the analyzers, using a 3-column Orsat analyzer charged with standard solutions for absorbing $CO_2$, $O_2$, and CO. Grab samples for $SO_X$ and $NO_X$ were obtained by means of the probe bundle that was not being used for infra-red and Orsat sampling. Before the sample was sucked into the evacuated vessel, the stainless steel tube was purged with a hand aspirator.

During each test, 3 $SO_X$ and 3 $NO_X$ grab samples were obtained by the method previously described. Before evacuation, each sample vessel was initially rinsed with absorbing solutions specific to each species, separated by distilled water rinses, and subsequently partially filled with a known volume of one of the solutions.

After collection, the sample was left in the vessel overnight, then the vessel pressure was measured and the solution was drained into a sample bottle; this was sealed and shipped to the Analytical Laboratory of the Ontario Ministry of the Environment. The samples were analysed colorimetrically and the results were reported as µg of $SO_4^{-2}$ and $NO_3^{-1}$ per ml of the respective absorbing solutions. The precision of the analyses was one µg/ml for $SO_4^{-2}$ and one µg/ml for $NO_3^{-1}$. From the volume of the absorbing solution and the pressure and volume of the gas sample, the results were converted to ppm $SO_X$ and $NO_X$.

Results

Measurements of $CO_2$, CO and $O_2$ are summarized in Table 8 for the 5 foundries at which the analyses were performed. The results for $CO_2$ and CO obtained by infra-red analysis consist of average concentrations for a single test. These were obtained by integrating the graphical result obtained at each sampling station, dividing the integral by the duration of sampling at each station, and then averaging the results over the complete test. The results obtained by Orsat analysis are compared with those obtained by the infra-red method by determining the ratio of the Orsat value to the instantaneous value measured by the infra-red sampler at the moment the Orsat sample was taken. The lack of precision of the Orsat method restricted comparisons of CO analyses to one foundry. $CO_2$ comparisons at 2 of the foundries were omitted due to an insufficient number of results.

A summary of $NO_X$ and $SO_X$ measurements for 5 of the foundries is presented in Table 9. Measurements were omitted for certain foundries when it was determined that the concentrations of $SO_4^{-2}$ and $NO_3^{-1}$ in the absorbing solutions were too low to permit accurate determination by the methods used.

No significant sources of variation could be identified for either $SO_X$ and $NO_X$ measurements. Significant variations in $CO_2$ and CO concentration occurred not only between foundries, but

Table 8

Summary of CO, $CO_2$ and $O_2$ Concentrations in Stack Gas

| Foundry | $CO_2$ | | | | CO | | | | $O_2$ |
|---|---|---|---|---|---|---|---|---|---|
| | $\bar{X}$, % | s, % | V, % | Orsat/Infrared | $\bar{X}$ % | s, % | V, % | Orsat/Infrared | Orsat, % |
| A | 5.1 | 0.6 | 11.8 | 0.95 ± 0.07 | 1.54 | 0.14 | 9.1 | 0.79 ± 0.17 | 13.5 ± 1.8 |
| B-1 and 2 | 7.6 | 0.5 | 6.6 | 0.96 ± 0.05 | 0.03 | 0.01 | 33.3 | N.A. | 12.3 ± 2.0 |
| B-ACD | 10.0 | 0.4 | 4.0 | | 0.04 | 0.01 | 25.0 | N.A. | |
| C | 8.2 | 1.3 | 15.8 | N.A. | 0.38 | 0.28 | 73.7 | N.A. | 13.0 ± 0.5 |
| D | 9.3 | 0.6 | 6.5 | 0.98 ± 0.07 | 0.73 | 0.24 | 32.9 | N.A. | 10.6 ± 1.7 |
| E-1 and 2 | 2.6 | 0.1 | 3.8 | N.A. | 0.50 | 0.35 | 70.0 | N.A. | 18.7 |

Table 9

Summary of $SO_X$ and $NO_X$ Concentrations in Stack Gas

| Foundry | Concentration of $SO_X$ | | | Concentration of $NO_X$ | | |
|---|---|---|---|---|---|---|
| | $\bar{X}$, ppm | s, ppm | V, % | $\bar{X}$, ppm | s, ppm | V, % |
| B | 710 | 208 | 29.3 | 11.9 | 1.0 | 8.4 |
| C | 481 | 123 | 25.6 | 33.0 | 9.6 | 29.1 |
| D | 288 | 155 | 53.8 | 22.0 | 6.4 | 29.1 |
| E | 276 | 143 | 51.8 | N.A. | N.A. | N.A. |
| F | 288 | 60 | 20.8 | 14.0 | 8.5 | 60.7 |

also within foundry B as a result of activation of the automatic charge door closing. Oxygen concentration varied significantly only between foundries.

As in the case of particulate emissions, variations in concentration of $CO_2$ and CO were observed within charge cycles. Although this phenomenon occurred to some extent at every foundry, it was especially evident at foundries A, C, and E. The nature and extent of these variations and concurrent variations in temperature are illustrated in Figure 5.

Excepting for foundries A and C, concentrations of $CO_2$ and CO did not vary significantly with probe position. At these foundries, however, significant variations were observed along the probe A axis as shown in Figure 6.

The reliability of gaseous emission measurements and other related parameters was assessed by means of the following methods:

1) carbon balance,

2) $O_2/CO_x$ ratios, and

3) dilution determinations.

The results of the measurement and comparison of carbon input and output at each of 4 cupolas are presented in Table 10. Variance analyses indicated that a significant difference between measured inputs and outputs occurred at only one cupola; this shows the data to be highly reliable.

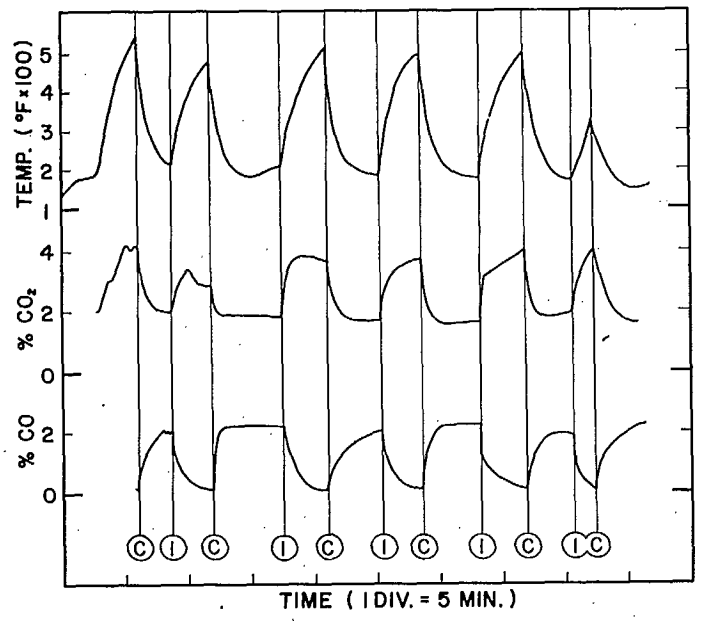


Figure 5. Variations in Temperature, CO and $CO_2$ Concentrations of Stack Gas during a Charge Cycle.

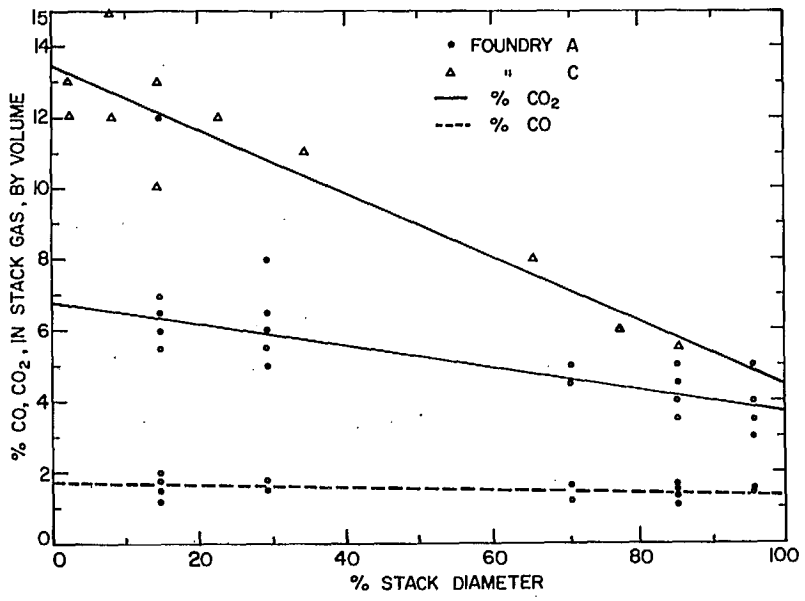


Figure 6. Variations in CO and $CO_2$ Concentration with Probe Position.

Table 10

Carbon Balance Results (1)

| Foundry | Carbon Input | Carbon Output | | | | Variance Analysis, Input vs. Output |
|---|---|---|---|---|---|---|
| | (Lb/Min) | $CO_x$ (Lb/Min) (2) | C (Lb/Min) (3) | Cp, (Lb/Min) (4) | Total (Lb/Min) | |
| A | 24.9 ± 1.4 | 24.1 ± 3.0 | 1.6 | 0.9 | 25.2 ± 3.0 | No Significance |
| B | 41.4 ± 2.7 | 44.1 ± 1.7 | 0.6 | 0.3 | 43.9 ± 1.7 | " " |
| D | 15.7 | 17.2 ± 2.2 | 0.4 | 0.1 | 16.9 ± 2.2 | " " |
| E-1 | 12.0 ± 0.7 | 14.7 ± 1.0 | 0.3 | 0.4 | 14.9 ± 1.0 | Difference Significant |
| E-2 | 15.4 ± 0.8 | 16.6 ± 1.0 | 0.3 | 0.4 | 15.8 ± 1.0 | No Significance |

(1) Excluding carbon in limestone.

(2) Because equal volumes of CO and $CO_2$ contain equal weights of carbon, no distinction was made between CO and $CO_2$ for this calculation.

(3) The column C describes the rate at which carbon is estimated to be taken into solution by the molten iron. The carbon content of the iron was assumed to increase by 0.3% for all foundries except foundry A where, due to the high percentage of steel charged, it was assumed to be 0.65%.

(4) The column $C_p$ describes the rate at which carbon was emitted from the cupola in the form of particulate. This quantity was determined by determining the weight loss incurred by ignition of the particulate samples.

The ratio between the concentration of oxygen and the sum of the concentrations of $CO_2$ and CO measured in the cupola stack above the charge door is uniquely defined by the oxygen: carbon ratio in the combustion zone and the ratio of dilution air to combustion gas at the point of measurement. The equations defining the appropriate concentrations are:

$$\% \ CO_x = (C_1 + C_2) \ / \ (1 + Z)$$

$$\% \ O_2 = (21Z - 0.5C_2) \ / \ (1 + Z)$$

where (1) $C_1$ and $C_2$ are concentrations of $CO_2$ and CO (expressed as volume %), respectively, in the undiluted exhaust gas and are uniquely defined by the oxygen:carbon ratio in the combustion zone;

(2) Z is the ratio of dilution air to undiluted exhaust gas at the point of measurement; and

(3) the assumption is made that CO is converted at the charge door to $CO_2$.

Because the degree of dilution Z cannot be determined at the point at which the $O_2/CO_x$ ratio is measured, the $O_2/CO_x$ ratio cannot be uniquely defined. However, the two equations define straight lines of constant oxygen:carbon ratio along which the $O_2/CO_x$ ratio is displaced by variations in Z. The internal consistency of the $O_2$ and $CO_x$ measurements can therefore be assessed by plotting individual ratios and comparing the points with the appropriate line defined by the oxygen-carbon ratio for the particular cupola, taken from Table 11. The results for the $O_2/CO_x$ ratio tests are shown in Figure 7.

Table 11 also summarizes the ratios of the average flow rates of the diluted and undiluted gases determined by two independent methods. The first method uses the ratio of the $CO_x$ concentration in the undiluted gas, calculated using the $O_2/C$ ratio, to the average $CO_x$ concentration taken from Table 8. The second method uses the ratio of the exhaust gas flow rate, taken from Table 3, to the air blast rate.

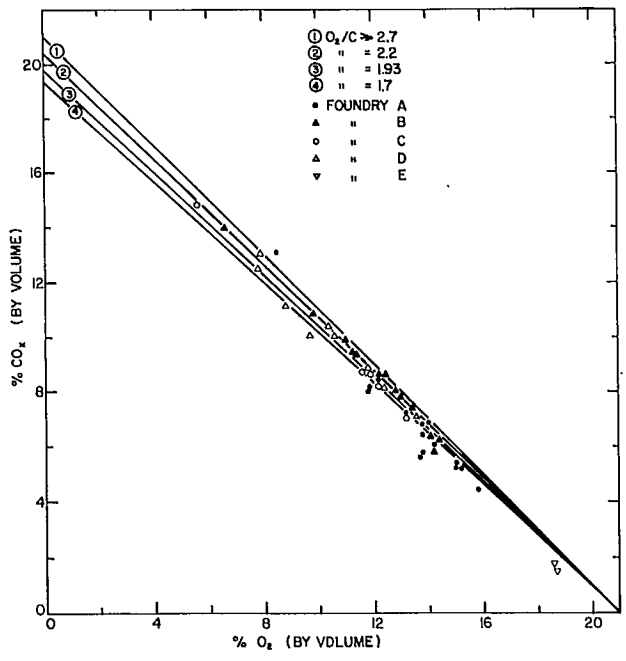


Figure 7. Calculated and Measured Relationships between % $O_2$ and % $CO_x$ in Cupola Stack.

Table 11

Dilution Analysis Results

| Foundry | Carbon Rate, (Lb/Min) | Blast Rate, (SCFM) | Exhaust Rate, (SCFM) | $O_2/C$ | $CO_2$ (%) (1) | CO (%) | $(CO_x)_{BCD}$ (%) (1) | $(CO_x)$ Stack % (1) | $(CO_x)$BCD / $(CO_x)$Stack | Exh.Rate / Blast Rate |
|---|---|---|---|---|---|---|---|---|---|---|
| A | 24.9 | 3080 | 11,700 | 2.17 | 15.5 | 9.2 | 24.7 | 6.2 | 4.0 | 3.8 |
| B-1 and 2 | 41.4 | 4550 | 18,500 | 1.95 | 12.3 | 14.2 | 26.5 | 7.4 | 3.6 | 4.1 |
| B-ACD | 41.2 | 4550 | 13,900 | 1.96 | 12.5 | 13.9 | 26.4 | 9.7 | 2.7 | 3.0 |
| D | 15.7 | 2875 | 5350 | 3.24 | 17.4 | 0 | 17.4 | 9.5 | 1.8 | 1.9 |
| E-1 | 12.0 | 1750 | 13600 | 2.50 | 19.3 | 2.8 | 22.1 | 3.0 | 7.4 | 7.8 |
| E-2 | 15.4 | 2110 | 17600 | 2.47 | 19.1 | 3.3 | 22.4 | 3.0 | 7.5 | 8.3 |

(1) Excludes $CO_2$ produced by calcination of limestone.

BCD means below charge door.

## Discussion

The results obtained by sampling cupola emissions in the stack above the charge door exhibit large variations. For all emission parameters measured, foundry-to-foundry variations were highly significant; however, a number of sources of significant variation were identified within the foundries tested. These variations were produced primarily by two sources: those associated with the inherent variability of a small cupola operation and those resulting from systematic changes in charging practice or cupola operation. Sampling errors were not a significant source of variation.

Reliable measurements of exhaust gas velocity and temperature are required not only to facilitate sampling of other emission parameters but to permit the correct design of abatement equipment. Average exhaust gas velocity is determined by the stack diameter, the air blast rate, the degree of dilution by charge-door air, and, to a lesser extent, by the air/coke ratio. It is not surprising, therefore, that differences in stack velocity are observed between cupolas having different air-blast rates, and different stack and charge door configurations. For a given cupola, variations in average stack velocity are produced by changes of the blast rate and by changes in the permeability of the charge material. Periodic blast rate measurements using Pitot tubes inserted in the blast ducting and the recording of periods of "wind-off" permitted the correlation of variations in stack velocity with changes in blast rate. The observation and recording of changes in charge make-up enabled the contribution of this factor to be assessed. The identification and assessment of these sources of variation facilitated the presentation in Table 3 of average "steady-state blast" stack velocities differentiated not only by foundry but also by operational changes. The use of this "significant source differentiation" resulted in coefficients of variation that were less than 10 per cent (Table 10).

The excellent agreement in both the carbon balance and the dilution analysis (Table 11) also confirm the accuracy of the average velocities and resultant blast rates.

Within a single test, stack velocity varies significantly with probe position at certain foundries. This variation results from several interrelated factors. The presence of down and upstream flow disturbances and the inability to avoid sampling in their zones of influence were responsible for significant variations with probe position at four foundries. The charge door dilution air is responsible for the systematic variation in velocity with position of probe A. Wall effects and, in the case of foundry A, a stagnant zone upstream from the center cone in a wet-cap caused the unusual profiles measured by probe B.

Average exhaust gas temperatures are controlled by factors such as air:coke and metal:coke ratios, burden depth, permeability, and dilution by charge door air. These factors are often unique to each cupola; therefore, the large foundry-to-foundry variations in average stack temperature can be understood, see Figure 2. However, Figure 2 also shows that, at many foundries, equally large variations occurred within a single test! Factors responsible are variations in burden depth due to irregular charging rates, intermittent ignition of CO at the charge door, and periods of "wind-off". The synergistic interaction between the effects of burden depth and CO ignition caused large variations in temperature but insignificant changes in velocity. Either deeper burden or the introduction of a fresh charge not only cooled the gases below the charge door but in doing so "quenched" the CO flame, causing a further decrease in temperature. Periodic intervals of "wind-off" caused variations in temperature only. Cooling of both the cupola and the burden during this period caused an initial reduction in gas temperature after resumption of full blast but had no influence on stack velocity.

These factors caused not only cyclic variations at a given test station - see foundries A, C, and E in Figures 3 and 5 - but also large variations within a test at all foundries, see Figure 2.

At foundries B and D which operate at high average stack temperatures,significant increases in stack temperature occur as melting progresses, probably as a result of reducing heat losses as the cupola becomes hotter. At foundry B, the gas temperature was increased significantly by the operation of the automatic charge door which reduced the amount of dilution air; see Table 11.

As in the case of stack gas temperature and velocity, particulate emission rates show highly significant variations between foundries. These, and the significant day-to-day variations observed at foundries A, B, C, and E result from variations in both charging practice and the nature of the materials charged. This relationship between charging practices and emission rates was demonstrated most clearly at foundries A and F which exhibited the highest and lowest emission rates, respectively. At foundry A, it was observed that large amounts of moulding sand were being returned to the cupola via a continuous conveyor belt system. The use of a screen to remove this loose sand halved the emission rates. Further efforts to exclude loose sand, rust, and coke breeze from the cupola further decreased the emission rates; see Table 6.

At foundry F, it was observed that the hand-charging procedures resulted in the exclusion of most loose rust and dirt from the cupola. This was confirmed on the last day of testing, when the test crew cleaned all the scrap charged, without reducing the emission rate.

The importance of loose dust in the charge as a contributor to particulate emissions was also emphasized in the results of the peak loading tests; see Table 5. The loose dust is blown up the cupola stack as soon as the charge is introduced, resulting

in dust-emission rates more than an order of magnitude higher than during the off-peak period. Though these variations may not be acceptable from an abatement aspect, they are not a direct source of variation in the integrated test result because a test consists of a relatively large number of cycles. High peak-loading rates can influence the measurement of dust emission rates if they are related to the daily average melting rate instead of to the charging rate during a test. Initially, the rates shown in Table 4 were calculated for the daily rates. Homologation according to the number of charges per test not only reduced variations but also shifted the mean values to those presently shown.

Comparing the variations shown in Table 4 and in Table 7 shows that sampling errors, even with deviations from isokinetic conditions as high as 20 per cent, are not a significant source of variation.

It should also be emphasized that the fuel system in a coke-fired cupola is essentially pure carbon and that no evidence of moisture was encountered over the entire test series. The difficulties associated with condensation of water vapour, such as sulfate precipitation and sampling volume error are absent.

The significant variations in CO, $CO_2$, and $O_2$ concentrations between foundries re-emphasize the differences in the design and operation of the cupolas tested. The absolute concentrations of these gases are affected primarily by the degree of dilution resulting from air drawn into the charge opening. The relative concentrations of CO and $CO_2$ depend not only on the degree of dilution but also on the stack temperature which controls the combustion of CO at the charge door. Variations in the degree of dilution at the charge door and the combustibility of CO also increased the variability of CO and $CO_2$ within certain foundries. At foundry B, the operation of the automatic charge door increased the concentrations of CO

and $CO_2$ but did not affect the $CO/CO_2$ ratio; this indicated a decrease in dilution only. The similar variations of both CO and $CO_2$ with the position of probe A at foundries A and C - see Figure 6 - suggest that a change in dilution is primarily responsible. However, the intermittent ignition of CO, observed at foundries A, C, and E, caused an increase in the variability of CO and $CO_2$, measured over a complete test, because unlike peak dust loading, cyclic CO combustion did not occur during every charge cycle.

Although $SO_x$ and $NO_x$ measurements exhibited large variations, no significant source could be identified. As a result, no conclusion can be made regarding the causes of variability of these gases. The sampling experience gained indicated that either improvements in grab sampling techniques or the use of continuous sampling methods should yield more accurate data.

The three methods used to test the reliability of the CO, $CO_2$, and $O_2$ analyses and related parameters such as blast rate, air/coke ratio, and stack gas flow rate yielded excellent results. Of the five cupolas tested for carbon balance, only one had a carbon output which differed significantly from the input. All $O_2/CO_x$ ratios showed little deviation from the calculated values. Exhaust:blast rate ratios, calculated from the ratio $CO_x$ measured above the charge door:$CO_x$ below the charge door (as calculated from air:coke ratio) agreed extremely well with air blast and stack flow rate measurements.

Summary to Part I

(1) Variations in cupola emissions between foundries are of such magnitude and significance that neither specific nor general emission measurements can be applied with any confidence to any foundry other than the one at which the measurements were taken.

(2) Variations within a foundry arise from a number of sources and are of such magnitude that testing should be conducted for several days if reliable results are to be obtained.

(3) Variation in stack gas temperature and velocity during a test necessitate the continuous measurement of these parameters.

(4) A relatively simple and robust particulate sampling train similar to the one described provides ample precision for cupola stack testing. Deviations from isokinetic sampling conditions as great as 20 per cent do not cause significant variations or bias in the particulate emission rate measurements.

(5) The gas analysis equipment and methods were reliable for the measurement of CO, $CO_2$ and $O_2$.

(6) The method of analysis for $NO_X$ and $SO_X$ should be improved or changed to provide greater precision and accuracy.

(7) The precision and accuracy of sampling practices are of limited value unless emission measurements are correlated with concurrent observations of cupola charging and operating procedures.

# PART II

# CHARACTERIZATION OF CUPOLA EMISSIONS

## Introduction

In Part I, the authors have attempted to define the reliability and practicability of a stack sampling method which they have used extensively over the past two years. In this part, the first problem is attacked through the detailed characterization of emissions from six iron foundry cupolas and the correlation of these characteristics with certain operating practices.

Comprehensive treatments of the problem of cupola dust emissions and their abatement, in compliance with regulations in Germany[2] and the United Kingdom[3], have been published recently. The wide variations in emissions documented in these papers emphasize the need for the accumulation of detailed information defining cupola emissions and correlating them, where possible, with cupola operating practices.

The results presented in this part were obtained during detailed studies of cupola emissions conducted at six iron foundries in the Province of Ontario. Daily testing programs were performed for two weeks at each of five foundries, and for one week at the sixth. Methods used to measure flow rate,

temperature, and composition of the stack gas and to collect particulate isokinetically are described in Part I. The collected particulate samples were sized, segregated into five size ranges, and subjected to X-ray diffraction and fluorescence analyses and loss-on-ignition determinations. The results were then correlated with cupola operating practices which had been observed simultaneously with emission sampling.

Cupola Operation Characteristics

All cupolas tested were of the cold-blast type and the melting and charging characteristics of each are summarized in Table 12. Not only did the type of iron and production rate differ at each foundry, but the size and type of casting ranged from small automotive castings at the malleable shop to large municipal castings at several of the grey-iron shops. Charging practice varied as much with the degree of control exercised as with the equipment. At certain foundries, this lack of control resulted in irregular charging rates, missed coke splits, and use of the cupola as a garbage incinerator as well as a melting device.

Charge make-up at the malleable and meehanite shops and at one of the other grey-iron shops was controlled to produce iron of a required composition. As a result, steel scrap, rail, and pig iron, along with foundry returns comprised the major proportion of each charge. Most of the particulates charged were loose and adhering moulding sand and rust. The inclusion of loose rust in the charge was especially obvious at foundry B, where an electromagnet was used to collect and make up charges. Significant amounts of sand were charged at foundry A because of the high proportion of sprues and gates and because of handling foundry returns by conveyor.

The less-stringent metal quality required at the remaining three foundries permitted more flexible charge make-up practices. At these foundries, the choice of scrap was primarily

TABLE 12

Melting and Charging Characteristics

| Foundry | Type of Iron | Nominal Production Rates Tons/hr (Tons/day) | Charge Rate (Measured) lb/min. | $O_2$/Carbon(5) (Metal/Coke) | Remarks |
|---|---|---|---|---|---|
| A | malleable | 8 (60-80) | 256 ± 13 | 2.17 (9:1) | Side dump charge bucket loaded by wheelbarrow. Charge - 60% returns (loose and adhering sand) 40% steel scrap -3 types: "ball" rusty, dense plate (1-2") less rust stampings-clean, low density |
| B | grey (1) | 8 (30-40) | 203 ± 16 | 1.95 (5.5:1 - 6:1) | "Orange Peel" charge bucket loaded by electro-magnet Charge - plate(clean), rail and pig (rusty), returns (sand-blasted) and auto scrap (dirt, grease & rust) |
| C | grey | 4.5 (10-15) | 150 (2) | (9.1) (2) | Side dump charge bucket loaded by hand. Charge - primarily domestic and auto scrap containing significant amounts of dirt, paint, rust and grease. |
| D | grey | 4.5 (20-25) | 147 (3) | 3.24 (9.1) | Cupola charged by wheelbarrows. Charge - 10% pig (very little rust), 25% returns (some adhering sand), 65% auto scrap (clean) |
| E-1 (4) -2 | grey | 3 ( 8-10) | 93 ± 8 116 ± 5 | 2.50 2.47 (9:1) | As Foundry C, exc. no auto scrap |
| F | grey | 3 ( 3-5) | 100 (2) | (9:1) (2) | As Foundry C, but scrap clean except for rust. Loose rust knocked off during hand loading of charge bucket. |

(1) Meehanite Licencee
(2) Charge weights estimated by foundry personnel.
(3) Charge weights variable, rate shown is average for test.
(4) -1, -2. refer to adjacent, identical cupolas.
(5) $O_2$ from air blast measurements.

dictated by economics and local availability, so the charge make-up depended primarily on the proximity of scrap to the charge bucket. Included with this scrap were significant amounts of paint, grease, dirt, and non-ferrous metals. Charge cleanliness at all foundries was observed to be influenced by irregular events such as a heavy rainfall or the clean-up of a dirty scrap bin.

Coke samples were selected at random at each foundry for proximate analysis and determination of calorific value. The results, shown in Table 13, are identical for each foundry within experimental error. Close control of the coke split was maintained at four of the foundries. At foundry B, for example, the metal/coke ratio was systematically decreased as melting progressed.

TABLE 13

Analysis of Coke

| Moisture % | Ash % | Volatile % | Fixed Carbon % | Sulphur % | Calorific Value BTU/lb |
|---|---|---|---|---|---|
| 0.53 | 7.76 | 1.22 | 90.49 | 0.62 | 13000 |

Dust Emission Characteristics

The dust emission characteristics of greatest concern to the cupola operator are the overall emission rate relative to the process rate, and the size distribution. The former characteristic indicates the degree of abatement required and the two together indicate the type of control equipment required. Though of less importance, the composition and morphology of the dust particles offer information not only on the origin but on the potential value and toxicity of the dust.

## Dust Emission Rates

The total dust emission rate for each foundry is shown in the first column of Table 14. Significant variations (by a factor of 10) occur not only between foundries but also within a given foundry. In addition to the "typical" continuous emission rates shown, experiments were conducted to relate the variation of emission rates to both charging practice and charge cycle. The details of these experiments are reported in Part I. At foundry A, the changes in charging practice were in steel scrap type and the removal of loose sand from foundry returns by a screen. The effects of changes in scrap type could not be separated from those of other variables; however, the use of the screen nearly halved the emissions. Further efforts to exclude loose sand, rust, and coke fines from the cupola further reduced the dust emissions. At foundry F, experiments confirmed that the hand-charging procedures excluded most loose dust from the cupola.

The importance of loose dust in the charge as a contributor to dust emissions was emphasized in the results of the peak loading tests. It was observed that loose charge-dust was carried up the stack as soon as the charge bucket was dumped. The dust emission rate, measured in the 30 seconds immediately following the introduction of a charge into the cupola, was as high as 7 times the average emission rate and 15 times the off-peak rate (see Part I).

## Dust Size Distribution

The size distribution of the dust emitted by the different cupolas was determined by means of standard screens as fine as 400 mesh and by optical and electron microscopic analysis of the minus 400-mesh fraction. The results are expressed incrementally and cumulatively in Figures 8 and 9 respectively. Of interest are the triple peaks at 0.5μ, 35μ, and 250μ and the absence of dust in the 1μ to 10μ range. Variations between foundries occur, primarily, in the size of the 0.5μ and 250μ peaks.

TABLE 14

Dust Emission Rate (lb/Ton of Metal Melted)

| Foundry | Total | Combustible | Non-Combustible | Bi | Pb | Zn | Fe | Mn | Ca | $SiO_2$* |
|---|---|---|---|---|---|---|---|---|---|---|
| A | 44.9 ± 13.5 | 5.7 ± 1.8 | 38.3 ± 10.9 | .27 ± .15 | .14 ± .11 | .11 ± .11 | 3.3 ± 1.6 | .65 ± .28 | .25 ± .16 | 31.5 |
| B | 15.5 ± 3.88 | 3.2 ± 2.0 | 1.25 ± 2.5 | .14 ± .14 | .26 ± .19 | .14 ± .05 | 2.55 ± 1.73 | .27 ± .10 | .61 ± .12 | 6.53 |
| C | 17.9 ± 7.33 | 6.2 ± 2.4 | 12.1 ± 4.8 | N.D. | .78 ± .21 | .55 ± .15 | 1.20 ± .60 | .15 ± .04 | .33 ± .14 | 7.76 |
| D | 8.2 ± 2.63 | 1.58 ± .58 | 6.4 ± 1.5 | N.D. | .31 ± .13 | .38 ± .11 | .68 ± .19 | .10 ± .04 | .14 ± .07 | 4.0 |
| E | 34.1 ± 9.40 | 8.5 ± 2.6 | 2.9 ± 8.6 | N.D. | 1.22 ± .15 | 1.67 ± .12 | 3.0 ± .14 | .34 ± .09 | .81 ± .44 | 18.7 |
| F | 4.8 ± 1.16 | 1.23 ± .17 | 3.55 ± .82 | N.D. | .31 ± .08 | .20 ± .02 | .4 ± .07 | N.D. | N.D. | 2.3 |

* $SiO_2$ emission rate was obtained by subtracting weight of O tied up in other metal oxides from fraction which consisted of elements too light for accurate fluorescence analyses. The assumption that it is primarily $SiO_2$ (quartz) is supported by X-ray diffraction.

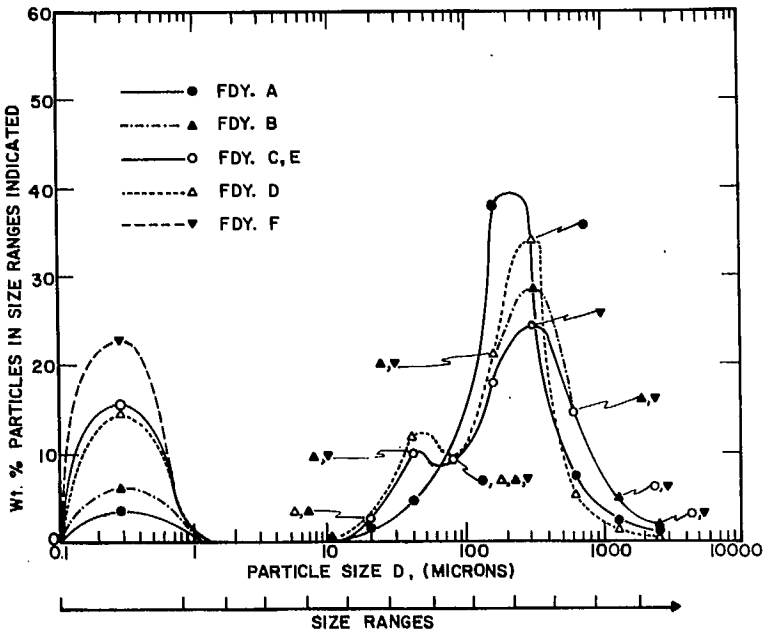


Figure 8. Incremental Dust Size Distribution

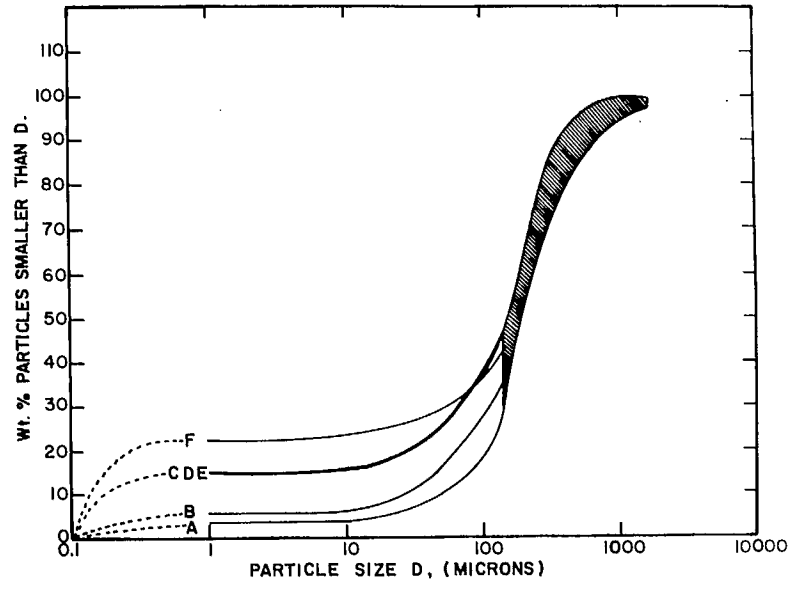


Figure 9. Cumulative Dust Size Distribution

Dust Composition

Dust composition for each cupola was determined by loss-on-ignition measurements and by X-ray fluorescence and diffraction analyses performed on samples segregated into five size ranges: +50-mesh (+297μ), -50 + 140-mesh (-297μ + 105μ), -140 + 270-mesh (-105μ + 53μ), -53μ + 1μ, and -1μ. X-ray analyses were performed on ignited samples by means of a Phillips Universal X-Ray Spectrometer. Initially, qualitative scans were conducted to determine the elements of interest. Quantitative determinations were then made using synthetic mixtures of Bi, Pb, Zn, Fe and Mn oxides and $CaCO_3$, in a $Al_2O_3$-$SiO_2$ matrix, as standards. X-ray diffraction studies were performed using a Guinier de Wolff monochromatic focussing camera. The resultant complex patterns were analyzed using a computer search program for the ASTM powder diffraction file. The use of the program was greatly facilitated by the determination of the elements present.

The average dust composition for each foundry, expressed as an emission rate for each element or component, is summarized in Table 14. Wide variations in emission rates occur between foundries for all elements and for the combustible and $SiO_2$ fractions of the dust. The emission rates of Pb, Zn, Fe, $SiO_2$, and combustible dust are of particular interest when compared with charging practices. The highest levels of Pb and Zn occur at foundries C and E in which the primary charge constituent is low-quality domestic or auto scrap. High iron-emission rates occur in foundries A, C, and E (rusty scrap) and foundry B (rusty scrap, electromagnetic charging). The predominance of $SiO_2$ in the emissions of foundry A confirms the importance, suggested previously, of charged moulding sand as a source of emission.

The combustible fraction of the dust probably consists of unburned coke and hydrocarbons. ("Afterburners" or "igniters" were turned off during sampling). Comparison of combustible

fractions for all foundries except B indicates the importance of dirt and grease in the scrap, since the metal:coke ratio is constant for these foundries. The high fractions of cumbustible at foundries C and E suggest that the amount of grease and dirt on the scrap is an important factor. The equally high combustible fraction of foundry A is explained by the observation that coke breeze was regularly swept up and shovelled into the charge bucket. Although foundry B has both a low metal:coke ratio and greasy auto scrap in the charge, the combustible emission rate is lower than the average (4.6 lb/ton) for the other 5 foundries. One possible explanation for this anomalous relationship between combustible emissions and coke input rate is the use of a drum cleaner for the charge-coke at foundry B. It was observed that this unit very effectively prevented coke fines from reaching the cupola.

Variations in emission rates with dust size are shown in Figure 10 for total and combustible dust, $SiO_2$, Fe, and Pb. Comparison of the total emission rates in each size range indicates that the greatest variations between foundries occur in the four coarser fractions of the dust, which consist mainly of dust transmitted by the cupola. The emission rate for the sub-micron dust, generated by the cupola as metallurgical fume, is relatively constant for all foundries except E which has a fume emission rate four times higher than the others.

Comparison of $SiO_2$ and total emission rates shows that for all size ranges at all foundries, $SiO_2$ is the primary constituent of the dust. Comparison of the combustible and total dust emission rates indicates that a significant and relatively constant fraction is combustible in the coarse fractions of the dust but this fraction become insignificant in the sub-micron dust. Similar distribution is exhibited by Fe, except at foundry A where Fe comprises a significant fraction of the sub-micron dust. Pb and Zn (not shown) display trends opposite to that of iron and combustible material; with the exception of foundries A and B, the lead content of the dust

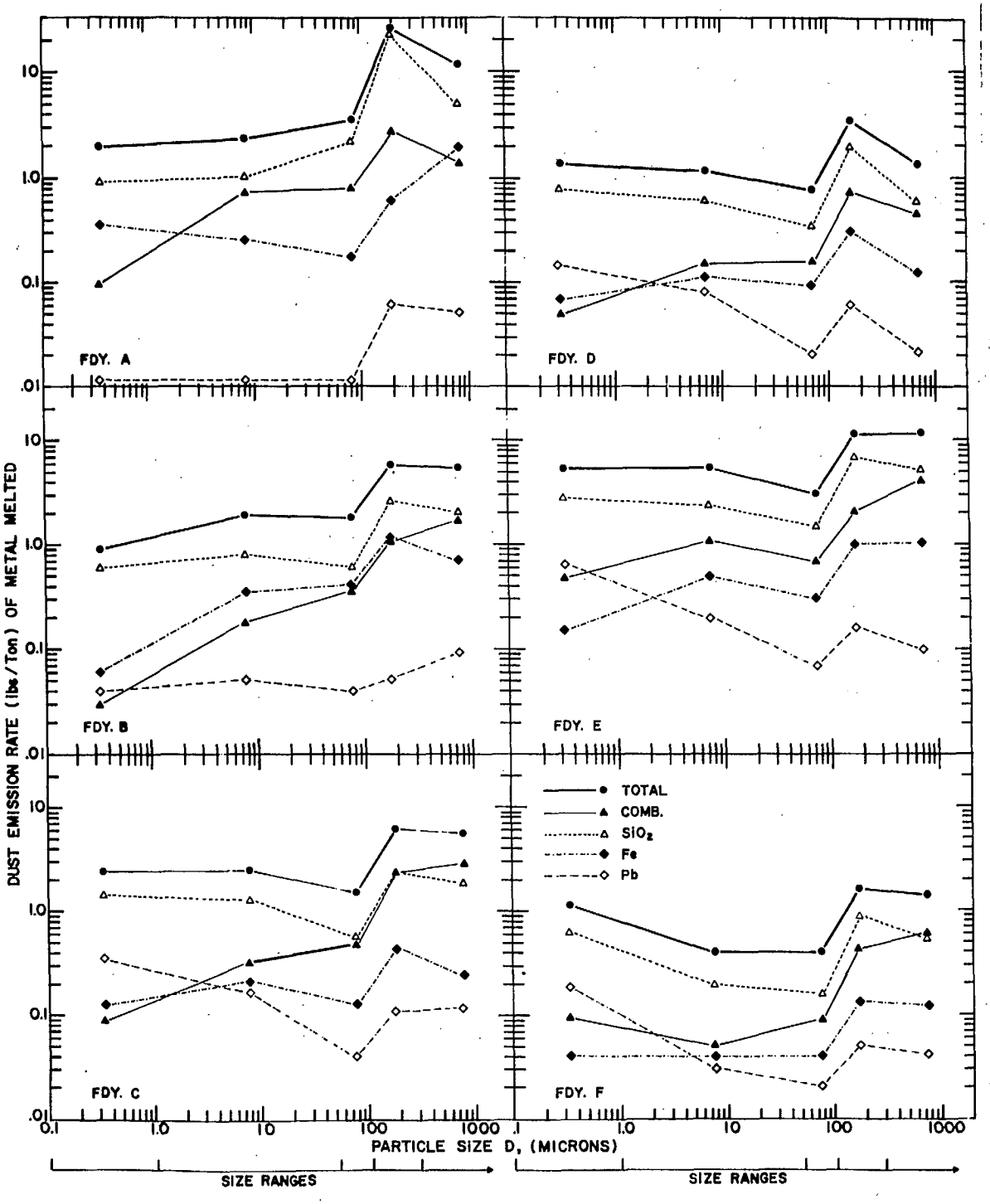


Figure 10. Dust Emission Rates for Various Sizes, Elements and Components

increases with decreasing dust size, attaining significant levels of emission and concentration in the sub-micron fraction.

The results of the diffraction analyses, summarized in Table 15, show that the compounds in which the principal elements are found do not vary significantly, either between foundries or between sizes coarser than one micron. In confirmation of the X-ray fluorescence results, $SiO_2$ (quartz) was the major constituent of the coarse dust at all foundries, $Fe_2O_3$ and $Fe_3O_4$ usually being minor constituents. Traces of refractory silicates and limestone were also detected at most foundries. A significant fraction of the sub-micron dust was found to be non-crystalline; fluorescence results suggest amorphous quartz or silicates. $Fe_2O_3$ and $Fe_3O_4$ were present in the sub-micron dust at most foundries, and PbS, $Pb_3O_4$, and ZnO were detected at foundries emitting high sub-micron concentrations of Pb and Zn.

Dust Morphology

A scanning electron microscope was used to determine dust morphology as a function of size for dust samples collected at each foundry. Results of the morphology analyses were identical for all the foundries; the only variation in particle shape occurred between the sub-micron dust and the coarser dust. Figure 11 illustrates that all sub-micron dust consisted of smooth spheres 0.1μ to 0.5μ in diameter. All dust coarser than one micron consisted of angular, irregularly shaped, particles (Figure 12). The demarcation between the two dust shapes was quite distinct. No angular sub-micron particles were observed; the only spherical particles observed in the coarse dust were sub-micron particles adhering to the surfaces of larger particles.

Gaseous Emission Characteristics

Reliable measurements of the cupola stack gas characteristics define not only the emissions but also the efficiency of the cupola operation. The gaseous emissions of greatest concern are the concentrations of CO, $SO_X$ and $NO_X$. Cupola efficiency

TABLE 15

Composition of Dust by Compounds

| Size Fraction | + 50 | -50 + 140 | -140 + 270 | -270 + 1μ | - 1μ |
|---|---|---|---|---|---|
| Foundry A | MR-$SiO_2$ | | | → | MR - $SiO_2$* |
| | T-$Fe_3O_4$ | | | ← MN-$Fe_2O_3$, $Fe_3O_4$ | MN-$Fe_2O_3$, $Fe_3O_4$ |
| | T-(Ca, Mg, Al)Silicates, $CaMg(CO_3)_2$ | | | → | |
| B | MR-$SiO_2$ | | | → | MR - $SiO_2$* |
| | MN-$Al_2O_3$ | | | → | MN - $Fe_2O_3$, $Fe_3O_4$ |
| | MN-$Fe_2O_3$, $Fe_3O_4$ | | | ← MR-$Fe_2O_3$, $Fe_3O_4$ | |
| | T-(Ca, Mg, Al) Silicates, $CaCO_3$ | | | → | |
| C | MR-$SiO_2$ | | | → | MR - $SiO_2$* |
| | MN-$Fe_2O_3$, $Fe_3O_4$, $CaSO_4$ | | | → | MN { $Fe_2O_3$, $Fe_3O_4$ |
| | T-(Ca, Mg, Al) Silicates, ZnO | | | → | PbS, $Pb_3O_4$ |
| | T-$CaMg(CO_3)_2$, $CaCO_3$, PbS | | | → MN → | |
| D | MR-$SiO_2$ | | | → | MR - $SiO_2$* |
| | MN-$Fe_2O_3$, $Fe_3O_4$, $CaSO_4$ | | | → | MN { $Fe_2O_3$, $Fe_3O_4$ |
| | T-(Ca, Mg, Al) Silicates, ZnO, PbO | | | → | PbS |
| E | MR-$SiO_2$ | | | → | MR - $SiO_2$* |
| | MN-$Al_2O_3$ | | | → | MN { ZnO, PbS |
| | T-(Ca, Mg, Al) Silicates, $Fe_2O_3$, $CaCO_3$ | | | → | $FeSiO_4$, $K_2SO_4$ |
| F | MR-$SiO_2$ | | | → | MR - $SiO_2$* |
| | MN-$Fe_2O_3$, $Fe_3O_4$ | | | → | MN { $Fe_3O_4$, $Pb_3O_4$ |
| | T-(Ca, Al, Mg) Silicates, ZnO, PbS/$PbSO_4$ | | | → | $CaCO_3$, $K_2SO_4$ |

MR = Major Compounds
MN = Minor "
T = Trace "

* The majority of the -1 micron $SiO_2$ was non-crystalline.

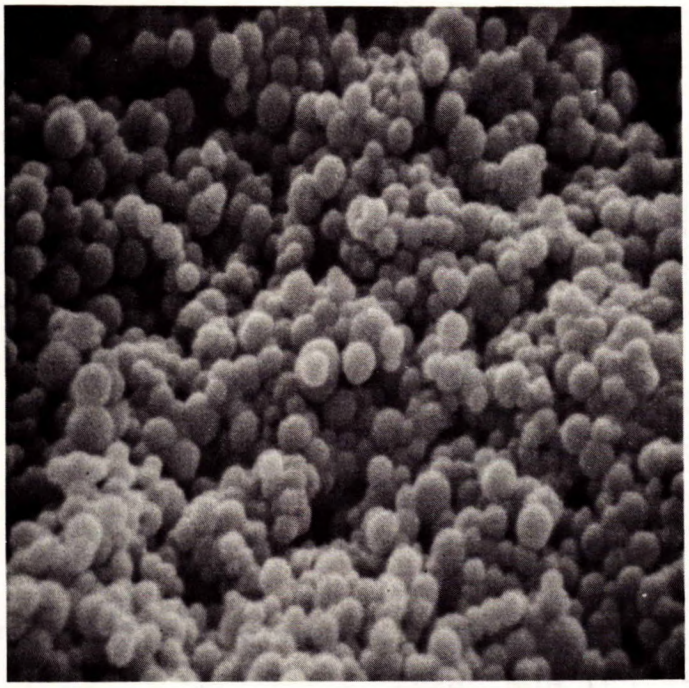

Figure 11. Sub-Micron Dust X23000

Figure 12. Coarse Dust X170

depends on the optimum combustion of coke, defined by the $CO/CO_2$ ratio, and on the amount of sensible heat lost in the stack gases. The flow rate and temperature of the stack gas are also of considerable concern to the abatement equipment supplier because these parameters define both the size and materials selection for the abatement equipment.

The flow rate, temperature and concentrations of CO and $CO_2$ in the stack gas were measured continuously. Concentrations of CO and $CO_2$ were also measured intermittently, as were the concentrations of $O_2$, $SO_x$, and $NO_x$. Details of the measurement procedures are reported in Part I. The gaseous emission characteristics for the six foundries are summarized in Table 16. The data presented are averages; the variability in the data is indicated by standard deviations, where sufficient measurements justified statistical analyses.

Before considering in detail the results presented in Table 16, it should be emphasized that they describe stack gas characteristics above the charge door; because of this, the effect of the air drawn into the stack through the charge door must be considered. Firstly, as indicated by the dilution factors shown in Table 16, the degree of dilution by the charge-door air is highly variable. At foundry D, a relatively small charge-door restricted the dilution factor to less than 2; at foundry E, however, a larger charge-door plus a negative pressure in the stack created by a large exhaust blower in the abatement system combined to produce a dilution factor of 8.

The importance of the air drawn in the charge-door, lies not only in the simple dilution effect, which increases the flow rate by an amount equal to the dilution factor and produces similar reductions in the concentration of $(CO + CO_2)$, $NO_x$ and $SO_x$, but in the resultant combustion of CO which affects both the $CO/CO_2$ ratio and the temperature of the stack gas.

TABLE 16

Gaseous Emission Data

| Foundry \ Stack Gas | Flow Rate SCFM | Temperature °F | CO Vol. % | $CO_2$ Vol. % | $O_2$ Vol. % | NOx ppm | SOx ppm | Dilution Factor (5) |
|---|---|---|---|---|---|---|---|---|
| A-1 (1) | 11,500 ± 710 | 325 ± 80 | 1.54 ± 0.14 | 5.1 ± 0.6 | 13.5 ± 1.8 | - | - | 3.8 |
| -2 | 9,800 - | 280 - | - | - | - | - | - | |
| -3 | 14,200 - | 400 - | - | - | - | - | - | |
| B-1 (2) | 18,500 ± 870 | 985 ± 70 | 0.03 ± 0.01 | 7.6 ± 0.5 | 12.3 ± 2.0 | 12 ± 1 | 710 ± 200 | 4.1 |
| -2 | | 1125 ± 65 | | | | | | |
| -ACD (3) | 13,900 ± 650 | 1250 ± 130 | 0.04 ± 0.01 | 10.0 ± 0.4 | | | | |
| C | 11,600 ± 990 | 1195 ± 350 | 0.38 ± 0.28 | 8.2 ± 1.3 | 13.0 ± 0.5 | 33 ± 10 | 480 ± 120 | N.A. (6) |
| D-1 (2) | 5,350 ± 520 | 1075 ± 220 | 0.73 ± 0.24 | 9.3 ± 0.6 | 10.6 ± 1.7 | 22 ± 6 | 290 ± 160 | 1.9 |
| -2 | | 1350 ± 180 | | | | | | |
| E-1 (4) | 13,600 ± 490 | 340 ± 165 | 0.50 ± 0.35 | 2.6 ± 0.1 | 18.7 - | - | 280 ± 140 | 7.8 |
| -2 | 17,600 ± 970 | | | | | | | 8.3 |
| F | 5,900 ± 400 | 725 ± 175 | - | - | - | 14 ± 9 | 290 ± 60 | N.A. (6) |

(1) -1, -2, and -3 refer to operation with plate, "ball" and stampings (Table 1)
(2) -1, -2, refer to chronological sequence of daily runs.
(3) -ACD refers to operation of automatic charge door.
(4) -1, 2, refer to adjacent cupolas.
(5) Dilution Factor = Exhaust Rate/Blast Rate.
(6) Blast Rate not measured.

The significant variability, not only between foundries, but within a given foundry, of the data in Table 16 is also worthy of comment. Variations between foundries in the stack flow rate can be accounted for by the variations in the melt rate, metal/coke and $O_2$/C ratios, and the dilution factor. Variations in the dilution factor are responsible for the variations in the concentration of $O_2$ and, in conjunction with variations in the $O_2$/C ratio, account for the variation in % ($CO + CO_2$) in the stack gas. However, the concentrations of $NO_x$ and $SO_x$, which should also be affected directly by the dilution factor do not vary with the dilution factor in a systematic manner. The possibility of significant sampling errors in both the $SO_x$ and $NO_x$ measurements makes further comment on their variability unjustified.

Variations in both the CO concentration and the stack gas temperature depend not only on the variability of the dilution factor but also on the propensity for ignition of the CO flame. The combustibility of the CO at the charge door increases with the concentrations of $O_2$ (dilution factor) and CO ($O_2$/C ratio) and the temperature of the undiluted stack gas, (metal:coke ratio and the efficiency of the cupola pre-heating zone). The low CO concentration and high stack temperature at foundry B result from a continuous CO flame caused by low metal:coke and $O_2$/C ratios and a relatively low burden height. Conversely, a deep burden, coupled with high metal:coke and $O_2$/C ratios at foundry A resulted in an intermittent CO flame, low stack temperatures and high CO concentrations. The CO combustion behaviours of the other four foundries were between those exhibited by foundries A and B.

Carbon and Heat Balances

Carbon balance calculations were made for foundries for which sufficient data were available in order to assess the reliability of the data. Heat balance calculations were also performed for these foundries to provide a comparison of stack

heat-loss rates with heat input rates. The results of these two sets of calculations are shown in Table 17. The application of a carbon balance to gaseous cupola data provides a means of assessing how accurately the data describe the cupola operation. The excellent agreement obtained in these calculations indicates that a high degree of sampling accuracy had been obtained, at least for those parameters used in the carbon balance.

Cupola efficiency should be of primary concern to the foundryman. Not only does an inefficient cupola consume more energy in the form of increasingly expensive coke but it also produces more combustion-related pollutants. With the installation of pollution abatement equipment, the foundryman must pay a double penalty for his cupola inefficiency. This inefficiency is often manifested by high stack gas sensible heat contents, so either the size or the complexity of the abatement equipment must be increased; this will increase capital and operating expenses. The stack loss data in Table 6 indicates that foundry A has a significantly lower stack loss and, therefore, should benefit not only from lower coke consumption but also from lower pollution control costs. The stack losses at the other foundries comprise more than one half of the total input and indicate that both emissions and melting costs can be reduced by changing cupola operating procedures.

TABLE 17

Heat Balance and Carbon Balance Results

| Foundry \ Variable | Carbon Input(1) lb/min | Blast Rate SCFM | $O_2/C$ | Heat Input BCD (2) BTU/min | Heat Input Total (3) BTU/min | Heat Output (Stack Gas)(4) BTU/min | Stack Loss % (5) | Carbon Output (Total) (1) lb/min |
|---|---|---|---|---|---|---|---|---|
| A | 25 | 3080 | 2.17 | 270,000 | 364,000 | 113,000 | 31.0 | 25 |
| B | 41 | 4550 | 1.95 | 373,000 | 597,000 | 354,000 | 59.0 | 44 |
| D | 16 | 2875 | 3.24* | 152,000** | 233,000 | 130,000 | 55.7 | 17 |
| E-1 | 12 | 1750 | 2.50 | 160,000 | 175,000 | 92,000 | 57.5 | 15 |
| -2 | 15 | 2110 | 2.47 | 196,000 | 218,000 | 119,000 | 54.5 | 16 |



* This exceptionally high ratio was obtained by dividing measured oxygen (blast) rate by measured coke rate; however, the cupola was operating satisfactorily. Orsat analyses below the charge door indicated a ratio of 2.00:1. It was observed that considerable quantities of air were by-passing the melting zone and re-entering the stack through cracks between the bricks at the charge door.

** using $O_2/C$ = 2.00:1

(1) Excluding C in limestone and metallic charge.

(2) Calculated from $O_2/C$ ratio. BCD = below charge-door

(3) From Coke, assuming all C $\rightarrow CO_2$.

(4) Includes latent + sensible heat.

(5) Stack Loss = (Heat Output)/(Total Heat Input) X100.

Summary to Part II

(1) Foundry-to-foundry variations in dust emission rates of almost one order of magnitude (45 lb/ton - 4.8 lb/ton) were observed. Significant variations were also observed within individual foundries.

(2) The largest variations in emission rate occur in the coarse fractions of the dust. Observations of charging procedures indicate this dust is transmitted, rather than generated, by the cupola and can be virtually eliminated by changes in charging practices.

(3) Emission rates for the sub-micron dust vary significantly only between foundries melting different types of scrap. Foundries melting primarily low-quality domestic and auto scrap emit up to four times as much sub-micron dust per ton of metal melted as foundries melting cleaner, higher-quality, ferrous scrap.

(4) Variations in emission rate with dust size results in different size distributions for the dust emitted by each foundry. These differences become significant below 100 microns. As a result, abatement of dust emissions will be more difficult at those foundries with a high proportion of fine dust, particularly if cumulative efficiency criteria are used.

(5) Silica is the predominant component of the dust in all size ranges. In the coarse dust, iron oxides and combustible species are also important. In the sub-micron dust, oxides of volatile metals such as lead and zinc become important.

(6) Two distinct dust particle morphologies were observed: sub-micron particles were spherical, indicating that they are metallurgical fume, and all coarser particles were angular.

(7) Gaseous emission characteristics varied between foundries. The factor primarily responsible for these variations was dilution by charge-door air.

(8) In addition to diluting the non-combustible gaseous components, the charge-door air significantly affects stack gas characteristics through the combustion of CO. At certain foundries, a continuous CO flame at the charge door resulted not only in extremely low CO concentrations but in high stack-gas temperatures.

(9) Carbon balance calculations indicated the measurements, pertaining to the carbon output of the stack gas, to be reliable.

(10) Heat balance calculations showed one foundry to have an acceptable stack loss, whereas the stack losses of the others were uniformly high. Excessive stack heat-losses exact a double penalty in not only increasing coke consumption but increasing emission abatement costs.

## REFERENCES

1) R. K. Jeffrey and G. K. Lee, "An Automated System for Continuous Monitoring of $CO_2$, CO and $O_2$ in Boiler Flue Gas". Mines Branch Technical Bulletin TB 115, September 1969.

2) W. Patterson, E. Weber and G. Engels. The British Foundryman, March 1972, p. 106.

3) F. M. Shaw. The British Foundryman, March 1972, p. 90.

ACKNOWLEDGEMENTS

The authors gratefully acknowledge the contribution made by the following people: Mr. R. G. Fouhse and his colleagues of the Canadian Combustion Research Laboratories, Mines Branch, in the field work involved in this investigation; members of the Metals Physics Section, Physical Metallurgy Division, for X-ray diffraction analyses and scanning electron microscopy; Mr. G. Lachance, Geological Survey of Canada, for X-ray fluorescence analysis; personnel from the Air Management Branch, Ontario Ministry of the Environment; and the personnel of the foundries involved in the program.

RDW/RKB/sg